



Cite this: *Chem. Commun.*, 2025, **61**, 2257

## Recent progress in electrochemical recycling of waste NdFeB magnets

Xuan Xu,<sup>id</sup>\*<sup>a</sup> Xiaozheng Jia,<sup>a</sup> Kunyuan Zhao,<sup>a</sup> Peng Xu,<sup>c</sup> Peng Jing,<sup>\*a</sup> Baocang Liu<sup>a</sup> and Jun Zhang<sup>\*ab</sup>

Neodymium iron boron (NdFeB) magnets are critical components in green energy technologies and have received increasing attention due to the limited availability of the raw materials, specifically rare earth elements (REEs). The supply risks associated with primary mining of RE ores, which have significant environmental impacts, underscore the necessity for recycling RE secondary resources. Waste NdFeB magnets, generated during manufacturing processes and recovered from end-of-life products, represent valuable RE secondary resources. Recycling these materials can ensure a reliable and sustainable supply of REEs. Compared to conventional metallurgical processes, electrochemical strategies offer advantages such as high efficiency, selectivity, ease of operation, and environmental friendliness. This review presents an overview of the current status and future prospects of electrochemical technologies for recovering RE metals, alloys, or compounds from waste NdFeB magnets. Special emphasis is placed on molten salt electrolysis and room-temperature electrolysis, including detailed reaction mechanisms involved in the recycling processes. Additionally, challenges and future strategies for the electrochemical recycling of waste NdFeB magnets, focusing on environmental impact evaluation, efficient recovery, and reduced reagent consumption are proposed.

Received 20th August 2024,  
Accepted 6th December 2024

DOI: 10.1039/d4cc04252b

rsc.li/chemcomm

### Introduction

With the increasing pressure and policy efforts to address global climate change, the green and low-carbon transitions represented by green energy technologies, such as wind power, photovoltaics, electric vehicles and efficient energy storage, have emerged as a global consensus.<sup>1</sup> For example, the International Energy Agency predicts that by 2030, the share of electric vehicles in global car sales will increase from approximately 5% to over 60%. Furthermore, by 2050, it is anticipated that 90% of global electricity production will derive from renewable energy sources, with wind and photovoltaic power generation accounting for 70%.<sup>2</sup> This global transition to green and low-carbon technologies will significantly drive the demand for critical metals, particularly rare earth elements (REEs), which are essential raw materials for low-carbon technologies such as wind power systems and electric vehicles.<sup>3</sup> Specific REEs, neodymium (Nd), praseodymium (Pr), and dysprosium (Dy) are crucial for manufacturing high-performance

permanent magnets used in these low-carbon technologies. These REEs utilized in Neodymium Iron Boron (NdFeB) magnets represent the largest application segment, accounting for 45% of total usage.<sup>4</sup> In 2022, global consumption of sintered NdFeB magnets reached 184 000 tonnes, and this consumption is projected to grow at an annual rate of 5.8%, reaching 322 000 tonnes by 2032 (Fig. 1(a)).<sup>4</sup> To meet projected demand in 2032, global supply for NdPr oxide needs to expand by 61 000 tonnes, based on a production level of 65 000 tonnes in 2022 (Fig. 1(b)).

To address the supply gap of NdPr, primary mining and ore processing of REEs may be considered as viable options. However, the distribution of rare earth (RE) reserves is characterized by a concentration in four main countries, with China holding the largest share of 44 million metric tons of rare earth oxides (REOs) equivalent, followed by Vietnam with 22 million metric tons, Brazil with 21 million metric tons, and Russia with 10 million metric tons, according to the U.S. Geological Survey.<sup>5</sup> Many RE exporting countries have imposed restrictions on the export of REEs due to their strategic importance, which has inevitably led to a supply crisis.<sup>6</sup> Moreover, the exploitation of RE mineral resources is not only energy-intensive and challenging to decarbonize, but also causes significant environmental issues. For example, the mining of 1 tonne of REEs generates approximately 2000 tonnes of toxic waste, including 75 m<sup>3</sup> of wastewater and 1 tonne of radioactive waste.<sup>7</sup> Therefore, global interest has been raised to produce REEs from secondary

<sup>a</sup> School of Chemistry and Chemical Engineering, Inner Mongolia University, Hohhot 010021, P. R. China. E-mail: xu.xuan@imu.edu.cn, pjing@imu.edu.cn, cejzhang@imu.edu.cn

<sup>b</sup> School of Chemistry and Environmental Science, Inner Mongolia Normal University, Hohhot, 010022, P. R. China

<sup>c</sup> SANY Heavy Industry Co., Ltd., Economic and Technological Development Zone, Changsha, 410100, P. R. China

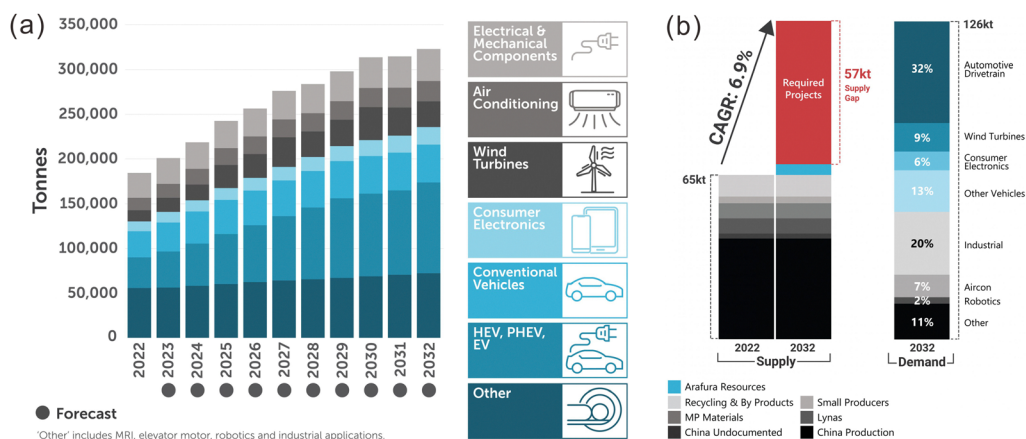


**Fig. 1** (a) Forecasting NdFeB magnet consumption by segment ('HEV, PHEV and EV' stands for hybrid electric vehicle, plug-in hybrid electric vehicle and electric vehicle, respectively). 'Other' includes Magnetic Resonance Imaging, MRI, elevator motor, robotics and industrial applications). (b) Global supply and demand forecast for NdPr in transition to green and low carbon. Report from Arafura Resources (<https://www.arultd.com/products/supply-and-demand.html>).

resources, such as the NdFeB magnet waste generated during the machining processes and spent NdFeB magnets from end-of-life (EoL) products, with the aim of establishing new circular supply chains. In fact, up to 50% of the raw materials are wasted as scraps/swarf/sludge at the magnet manufacturing sites, while the overall recycling potential of spent NdFeB magnets in the European Union from 2018 to 2040 is estimated to be 25 700 tonnes.<sup>8</sup> Thus, the anticipated gap between demand and supply of NdPr may be partially alleviated through the recycling of these waste NdFeB magnets, thereby integrating REEs into the circular economy.

The chemical composition of the NdFeB magnets varies across different applications. Generally, NdFeB magnets incorporate 20–30 wt% of REEs, primarily neodymium (Nd) and praseodymium (Pr), with minor additions of dysprosium (Dy) and/or terbium (Tb), and over 60 wt% of iron (Fe).<sup>9,10</sup> From a microstructural perspective (Fig. 2(a)), NdFeB magnets typically consist of three equilibrium phases: the hard magnetic matrix phase ( $\text{Nd}_2\text{Fe}_{14}\text{B}$ ), the minor boride phase ( $\text{NdFe}_4\text{B}_4$ ) and the RE-rich grain boundary phase (composed of metallic Nd and  $\text{Nd}_2\text{O}_3$ ).<sup>11</sup> It should be noted that the term "magnet scraps" is used variably in the literature to refer to different sources of magnets. In this paper, the extracted NdFeB magnets from the

EoL products and the off-quality NdFeB magnets generated in the manufacturing process are collectively referred to as "NdFeB scraps". The wet NdFeB magnet sludge, a mixture of oil, machining chips, and other solid residue, generated during the grinding and polishing processes is termed as "NdFeB swarf" (Fig. 2(b)).

## Challenges of current recycling methods for waste NdFeB magnets

The effectiveness of recycling methods for waste NdFeB magnets (whether scrap or swarf) varies significantly depending on the type of waste. A general schematic representation of the recycling process for waste NdFeB magnets is illustrated in Fig. 3. As the NdFeB magnet scraps are slightly contaminated and oxidized/corroded, a direct re-use of these magnet wastes in their entirety is currently regarded as the most ecologically and economically favourable approach due to the minimum energy consumption in a very short loop without waste generation. This magnet-to-magnet routes, such as re-sintering process<sup>13</sup> and hydrogenation disproportionation desorption and recombination (HDDR) process,<sup>14</sup> ends up with new magnets that can be reintegrated into the same systems or applications. However, since NdFeB magnet scraps are completely

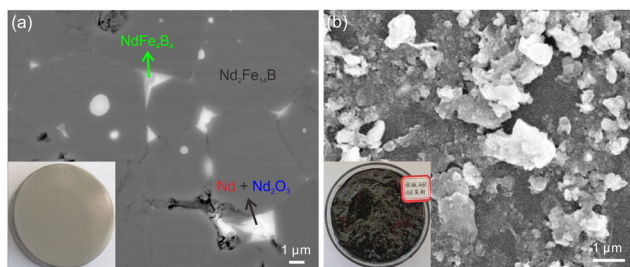


**Fig. 2** SEM images of (a) NdFeB scrap and (b) NdFeB swarf (after removing the grinding oil) with insets showing optical images. Reproduced with permission from ref. 11 and 12.

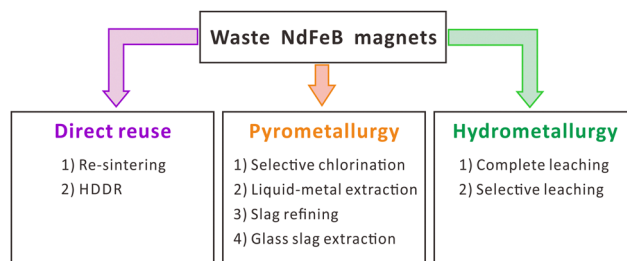


**Fig. 3** Schematic of general process for treatment of waste NdFeB magnets.

reused without separating the non-ferromagnetic phases, *e.g.*, RE oxides, the overall volume of these non-ferromagnetic phases increases with successive recycling cycles. As a result, the magnetic properties of NdFeB magnets produced from these repeated recycling processes tend to deteriorate as the number of recycling cycles increases.<sup>8</sup> Consequently, the magnet industry still prefers to manufacture magnets using fresh raw material to ensure desirable magnetic strength.

To date, many studies have reported the extraction of critical raw materials from waste NdFeB magnets in the form of RE salts/oxides/alloys, using either pyrometallurgical or hydrometallurgical processing route. A variety of pyrometallurgical processes, including selective chlorination method,<sup>15,16</sup> liquid-metal extraction,<sup>17,18</sup> slag refining<sup>19</sup> and glass slag method,<sup>20,21</sup> are detailed in the literature for recycling waste NdFeB magnets. In general, the pyrometallurgical processes are applicable to all types of waste NdFeB magnets, offering high treatment capacity while requiring minimal water usage, making them suitable for regions with limited water resources. However, pyrometallurgy involves high-temperature processes, necessitating significant energy input and leading to losses of REEs. Moreover, the use of non-recyclable and/or unstable chemicals, along with the generation of considerable solid waste, pose substantial environmental challenges. Hydrometallurgy is practically the main processing technique in the industry for recovering REEs from waste NdFeB magnets in the form of RE fluorides/oxides. The hydrometallurgical recycling of waste NdFeB magnets is applicable to both slightly and heavily oxidized magnet materials with diverse compositions. Acid leaching represents a critical step, as it significantly influences the extraction efficiency of REEs, their concentrations in the leachate, and selectivity against contaminants, such as Fe, which needs to be minimized during the precipitation of REEs. To date, two different leaching routes have been established: a complete leaching route and a selective leaching route. Currently, the oxidative roasting-selective leaching process, *i.e.*, HCl-preferential dissolution method is widely implemented in industrial production in China for REE recovery from waste NdFeB magnets.<sup>22</sup> This method is commercially attractive thanks to the appropriate consumption of acids and alkalis compared to the complete leaching route.<sup>23</sup> As the hydrometallurgical recycling route is quite similar to the existing hydrometallurgical processing of ores for REEs, the RE-rich leaching solutions can be integrated into an existing RE separation plant following the removal of non-REEs.<sup>24</sup> The separated REOs or fluorides (REF<sub>3</sub>) obtained through hydrometallurgical processes inherently exhibit a substantial environmental footprint because of the significant consumption of strong mineral acids and alkalis, along with the generation of considerable wastewater.

Conventional pyrometallurgical and hydrometallurgical technologies involve high-temperature processing, lengthy process flows, pollutant emissions, equipment corrosion, and costly chemical consumption. In contrast, electrochemical metal recovery is an emerging field offering a sustainable approach for extracting valuable metals from industrial wastes.

Based on fundamental investigations into alloy corrosion phenomena<sup>25,26</sup> and the electrochemical dissolution of ores and minerals,<sup>27,28</sup> electrochemical extraction and recycling systems have been progressively developed to address industrial wastes and urban mining challenges. Electrochemical processes transport electrons from the anode (where oxidation reaction occurs) to the cathode (where reduction reaction occurs) by applying voltage between the electrodes without the need for significant toxic chemical inputs. Therefore, the recycling of waste NdFeB magnets through etching or even complete leaching can be achieved *via* oxidation reactions at the anode, with simultaneous deposition of metals or alloys at the cathode. These electrochemical processes have the advantages of environmental compatibility, broad tunability, and minimal chemical usage, all of which may alter the current waste NdFeB magnets recycling route and efficiently promote the recovery of REEs from more complicated industrial waste streams. This paper systematically summarizes the current status and recent advances in electrochemical recycling of waste NdFeB magnets, focusing on molten salt electrolysis and room-temperature electrolysis. Emphasis is placed on the fundamental studies of redox reaction design at both the anode and cathode, as well as the mechanisms involved. Additionally, the challenges and future perspectives of electrochemical recycling technology are expounded in detail. The objective of this paper is to provide a comprehensive understanding of the state-of-the-art electrochemical recycling strategies and future directions for waste NdFeB magnets and to provide a general guideline for the electrochemical treatment of industrial wastes.

## Molten salt electrolysis

Molten salt possesses high ionic conductivity and wide electrochemical windows, making it an excellent electrolyte for extracting and refining metals/alloys. Molten salt electrolysis is extensively employed for electrolytic reduction of metal salts/oxides to metals/alloys. Notably, molten salt electrolysis is the predominant industrial technique to obtain approximately 80–90% of RE metals, including Ce, La, Nd, and Pr.<sup>29</sup> The recovered RE metals/alloys hold potential for integration into existing NdFeB production line, thereby streamlining the recycling process from waste magnets to new magnets.

### REE dissolution by direct anodization

Due to the variation of the electrochemical potential of Nd/Nd<sup>3+</sup> (−2.32 V *vs.* standard hydrogen electrode, SHE), Fe/Fe<sup>2+</sup> (−0.447 V *vs.* SHE) and B/H<sub>3</sub>BO<sub>3</sub> (−0.89 V *vs.* SHE),<sup>30</sup> the REEs can be, theoretically, leached away selectively through electrochemical anodization by controlling the potential and maintaining it in the region where the dissolution of the REEs occurs while the metallic Fe, B and other elements are stable or immune. The overall recycling route based on anodic dissolution for waste NdFeB magnets in molten salts is illustrated in Fig. 4.

Kamimoto *et al.*<sup>31</sup> investigated the electrochemical leaching behaviour of various elements in sintered NdFeB magnet scraps

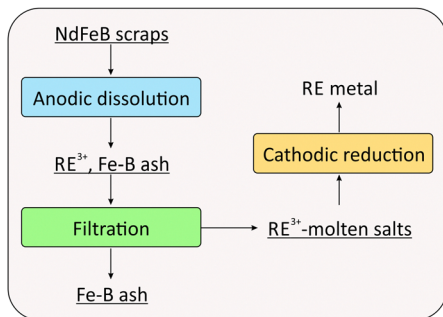
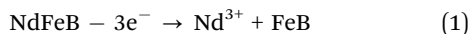


Fig. 4 Schematic of the overall recycling route based on anodic dissolution for waste NdFeB magnets using molten salt electrolysis.

using a molten bath consisting of 59 mol% LiCl + 41 mol% KCl at 723 K. Potentiostatic electrolysis enabled the selective leaching of REEs from the magnet within a potential range from  $-1.8$  to  $-0.8$  V (vs. Ag/AgCl). Controlling the oxidation potential allowed for the regulation of the oxidation stage during potentiostatic electrolysis. In the first stage, the REEs were leached from the grain boundary phase of the magnets. In the second stage, the REEs were leached from the interior of the  $\text{Nd}_2\text{Fe}_{14}\text{B}$  matrix phase, leaving metallic FeB as a residue. Therefore, the oxidation reaction of the NdFeB magnet scrap on the anode could be expressed by eqn (1):



Although the estimated leaching ratio of the REEs was approximately 90% at controlled potentials, the oxidation reaction of Fe (eqn (2)) could not be avoided because of the limited diffusion rate of REEs from the interior of the NdFeB magnet scrap to its surface.<sup>32</sup> Additionally, the dissolved RE in the electrolyte was deposited on the liquid Zn cathode to form RE-Zn alloys with the current efficiency up to 91.5%.<sup>33</sup>

To enhance the diffusion of REEs during anodic oxidation, Yang *et al.*<sup>34</sup> proposed an idea of forming anode channels within the RE permanent magnets (REPMs), specifically NdFeB magnet scrap, which was directly used as the anode in a molten LiF-CaF<sub>2</sub> bath at 1123 K (Fig. 5(a)). These channels could provide continuous transport paths between the electrolyte and the REEs inside the electrode, thus promoting the oxidation of REEs that did not diffuse to the surface of the NdFeB magnet. Cyclic voltammetry (CV) was employed to investigate the redox reactions of the NdFeB magnet electrode, confirming the oxidation peaks of both the RE-rich phase and the REEs in the  $\text{Nd}_2\text{Fe}_{14}\text{B}$  phase. By applying currents on the NdFeB magnet anode, pores and channels were formed due to the oxidation of the RE-rich phase, while the observed micropores could be ascribed to the dissolution of REEs in the  $\text{Nd}_2\text{Fe}_{14}\text{B}$  phase. The selectively dissolved RE ions in molten LiF-CaF<sub>2</sub> salts were directly deposited on the cathode as RE metals, while other elements were left in the form of Fe and Fe<sub>2</sub>B. Although the pores and channels improved access between the electrolyte and REEs within the REPM electrode, the dissolution of Fe from the REPM electrode still could not be completely avoided.

Konishi *et al.*<sup>35</sup> proposed a novel process that utilized an alloy diaphragm in a molten LiCl-KCl (45:55 wt%) salt at 723 K. A rare earth-transition metal (RE-TM) alloy served as the diaphragm, functioning as a bipolar electrode and facilitating the selective “permeation” of the RE ions (Fig. 5(b)). The recovery of RE metals or alloys involved the following steps: (i) a REE-containing material, such as sintered NdFeB magnet scrap, is used as the anode, causing the selective dissolution of RE metals into the melt as ions; (ii) the dissolved RE<sup>3+</sup> ions are reduced at the anode side surface of the diaphragm while REE atoms diffuse through the diaphragm; (iii) REE atoms are dissolved from the cathode side surface of the diaphragm as ions, and (iv) REEs are ultimately recovered as metals or alloys on the cathode by the reduction of the dissolved RE<sup>3+</sup> ions. The RE<sup>3+</sup> ions in the anode compartment can be collected by

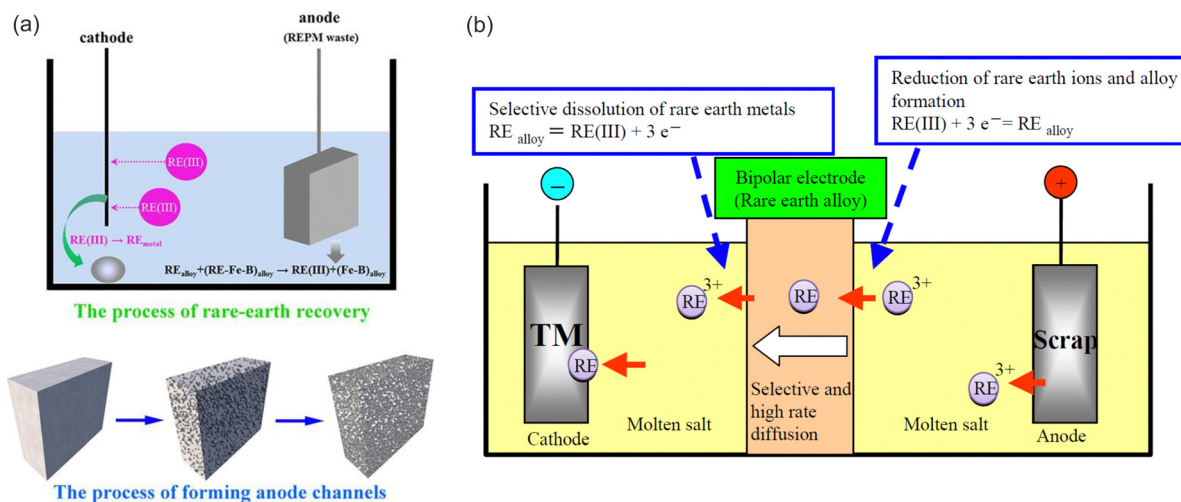


Fig. 5 (a) Illustration of REEs recovery from REPMs by molten salt electrolysis. (b) The process for separation and recovery of the REEs from a NdFeB magnet scrap using a bipolar electrode. Reproduced with permission from ref. 34 and 35.

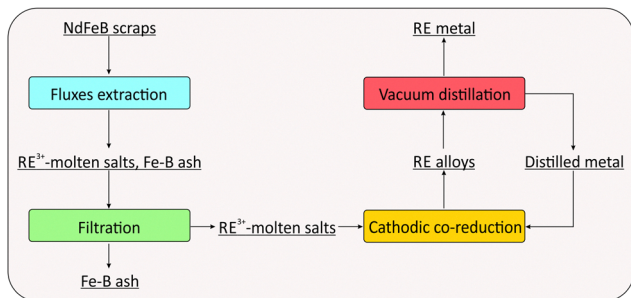


Fig. 6 Schematic of the overall recycling route based on fluxes extraction for waste NdFeB magnets using molten salt electrolysis.

electrolysis using an additional cathode. Almost all impurities remain in the anode compartment as residue or anode slime. This process has the potential to recover highly pure RE materials or even allows the selective recovery of the RE metals like Dy from sintered NdFeB magnet scraps because of the high selectivity during the alloying step on the anode side surface of the diaphragm. On the other hand, some technical problems remain unresolved, including the low mechanical strength of the RE-TM alloys and difficulties in maintaining the alloy diaphragm at an optimal composition. Thus, further investigations are required to determine the commercial applicability of this process.

### REE extraction by fluxes

An alternative method to anodic dissolution for separating REEs from waste NdFeB magnets involves the reaction between REEs and fluxes. The commonly used fluxes, metal chlorides<sup>36,37</sup> (e.g.,  $\text{AlCl}_3$  and  $\text{MgCl}_2$ ) and fluorides<sup>38</sup> (e.g.,  $\text{AlF}_3$ ,  $\text{ZnF}_2$  and  $\text{FeF}_3$ ) selectively react with REEs in the magnets to form RE halides, while Fe remains unreacted in the molten salts. The extraction mechanisms of REEs in chloride and fluoride fluxes are similar. For instance, the reactions and Gibbs free energies associated with  $\text{AlF}_3$  are summarized by eqn (3)–(7):<sup>38</sup>



The resulting RE halides can be reduced at the cathode to form RE metals. However, metal ions from the fluxes, such as Al, Mg, Zn and Fe are preferentially reduced due to their more positive reduction potentials compared to  $\text{RE}^{3+}$  ions, leading to the co-reduction of RE alloys at the cathode. This co-reduction process avoids the comproportionation of  $\text{Nd}^{2+}$  ( $2\text{Nd}^{3+} + \text{Nd} \leftrightarrow 3\text{Nd}^{2+}$ ),<sup>39</sup> which commonly occurs during electrolysis, thereby enhancing the electrical efficiency. On the other hand, further separation of REEs from these alloys, such as vacuum distillation,<sup>40</sup> is required if pure RE metals are the ultimate target. It is important to note that vacuum distillation, which

relies on differences in the saturated vapor pressures of metals,<sup>41</sup> is an energy-intensive process that increases the overall cost of recycling. Additionally, the current RE electrolysis industry favors fluoride electrolysis over chloride electrowinning due to the hygroscopic nature and vaporization issues of chlorides.<sup>42</sup> Nevertheless, the overall recycling route based on flux extraction for waste NdFeB magnets using molten salt electrolysis is illustrated in Fig. 6.

Hua *et al.*<sup>43</sup> investigated the use of  $\text{MgCl}_2$ – $\text{KCl}$  molten salts for the selective extraction of REEs from NdFeB scraps. The extraction process was proposed as follows: initially, the REEs on the surface of the granulated magnet scrap reacted with molten  $\text{MgCl}_2$ , leaving behind FeB residue that formed an ash layer, while the reaction products penetrated the bulk molten chlorides. During the chlorination process, the  $\text{MgCl}_2$  in the bulk melts diffused through the ash layer to the surface of unreacted scrap, facilitating the extraction of REEs, while the reaction interface was moving gradually toward the core of magnet scrap. Consequently, the ash layer thickened and the size of the unreacted scrap core decreased until the reaction was complete, as illustrated in Fig. 7. Approximately 90% of the REEs in the scrap could be extracted into molten chlorides by keeping contact with the molten  $\text{MgCl}_2$ – $\text{KCl}$  (0.6 : 0.4 mol%) at temperatures ranging from 1000 to 1200 °C for more than 10 h. To achieve selective extraction of REEs from NdFeB scraps at lower temperatures and shorter reaction times with higher efficiency, molten  $\text{CdCl}_2$ – $\text{LiCl}$ – $\text{KCl}$  was utilized.<sup>44</sup> With sufficient content of  $\text{CdCl}_2$ , over 99% of Nd could be selectively extracted into the molten salts within 2 h at a temperature of 773 K, while Fe and B remained in the solid phase. Additionally, the correlations between  $\text{CdCl}_2$  content and cyclic voltammetry data were utilized to monitor the reaction progress and determine the extraction endpoint in real-time. Abbasalizadeh *et al.*<sup>45</sup> further demonstrated that REOs in molten fluorides could be converted into  $\text{REF}_3$  with the addition of fluorinating agents such as  $\text{AlF}_3$ ,  $\text{ZnF}_2$ ,  $\text{FeF}_3$  and  $\text{Na}_3\text{AlF}_6$  prior to electrolysis (eqn (8)–(11)). The resulting  $\text{REF}_3$  can subsequently be processed through electrolysis in the same reactor to extract RE

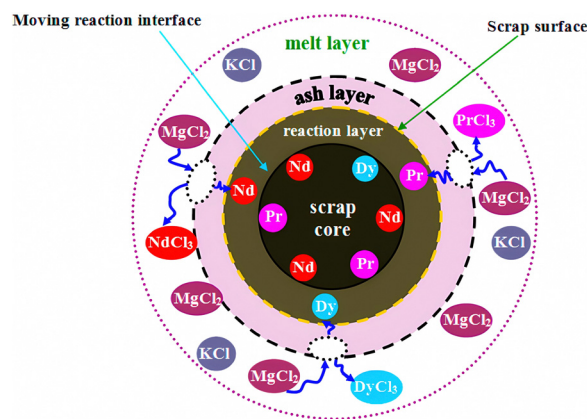
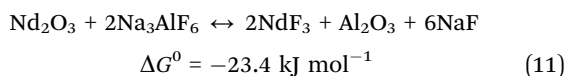
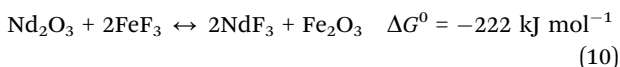
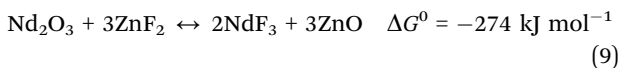
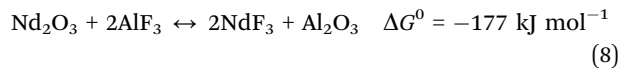


Fig. 7 Schematic diagram of the unreacted shrinking core model for the extraction of REEs from NdFeB scraps using molten  $\text{MgCl}_2$ – $\text{KCl}$  salts. Reproduced with permission from ref. 43.

alloys as the cathodic deposits. This finding indicates that molten salt electrolysis, coupled with flux extraction is effective for recycling heavily oxidized NdFeB swarf in addition to NdFeB scraps.



Although the recycling of waste NdFeB magnets through molten salt electrolysis results in RE metals/alloys that can be directly utilized as raw materials in the production of new NdFeB magnets. This process significantly reduces the steps involved in recycling compared to conventional hydrometallurgical methods. However, the separation of individual REEs from the RE metals/alloys necessitates additional efforts to expand their applications beyond NdFeB magnets. Furthermore, molten salt electrolysis operates at high temperatures, which not only demands substantial energy but also presents significant technical challenges in precisely controlling the composition of the molten salts, which is an essential factor for the effective dissolution of waste NdFeB magnets.

## Room-temperature electrolysis

Room-temperature electrolysis, characterized by minimal chemical input and mild operating conditions, offers a sustainable and environmentally friendly strategy for resource recovery through the electrochemical oxidation or reduction of valuable metals. Specifically, electrochemical oxidation provides a selective and green approach for the treatment of industrial waste by applying an external voltage to the anode, facilitating the dissolution of valuable metals.

### Direct anodic dissolution

NdFeB magnet scraps, being highly conductive, can be directly used as the anode for electrochemical leaching, thereby bypassing energy-intensive processes such as crushing, grinding, and roasting. It should be noted that the microstructure of the NdFeB magnet scraps plays a crucial role in their dissolution mechanisms. Generally, NdFeB magnets consist of  $\text{Nd}_2\text{Fe}_{14}\text{B}$  grains (the matrix phase, accounting for 85–87% of the whole magnet),<sup>46</sup> surrounded by a RE-rich phase and a B-rich phase in the grain boundaries. The RE-rich phase corrodes preferentially due to the negative standard reduction potential of REEs, followed by the dissolution of the B-rich phase, which may even lead to the pulverization of the magnet.<sup>47–49</sup> Thus, recovering  $\text{Nd}_2\text{Fe}_{14}\text{B}$  matrix grains as raw material for new magnet production could be a viable alternative to direct reuse method.

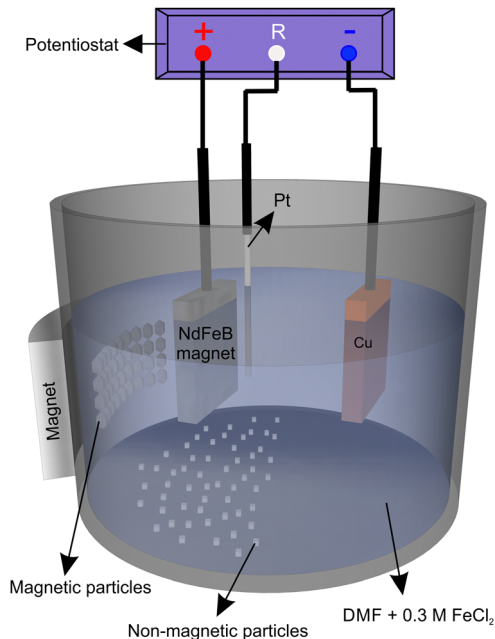
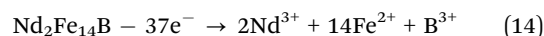
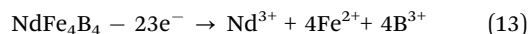


Fig. 8 Schematic illustration of the electrolytic cell for recovering the  $\text{Nd}_2\text{Fe}_{14}\text{B}$  grains from the sintered NdFeB magnets. Reproduced with permission from ref. 11.

Xu *et al.*<sup>11</sup> developed an electrochemical etching process that selectively dissolved the RE-rich grain boundaries of a NdFeB magnet scrap in an organic *N,N*-dimethylformamide (DMF)– $\text{FeCl}_2$  electrolyte at room temperature (Fig. 8). By fine-tuning of the applied anodic current density to less than  $5 \text{ mA cm}^{-2}$ , the selective dissolution priority of the phases inside the magnets is as follow: metallic Nd > intergranular  $\text{NdFe}_4\text{B}_4$  > matrix  $\text{Nd}_2\text{Fe}_{14}\text{B}$  (eqn (12)–(14)).



Therefore, RE metal in the grain boundaries could be preferentially dissolved, leaving behind the  $\text{Nd}_2\text{Fe}_{14}\text{B}$  grains and RE oxides for magnetic separation. At the anodic current density of  $2 \text{ mA cm}^{-2}$ , 67.2% of the NdFeB magnet was recovered as  $\text{Nd}_2\text{Fe}_{14}\text{B}$  grains with an energy consumption of only  $0.58 \text{ kW h kg}^{-1}$ . The mechanism study of the electrochemical etching process suggested that the recovery of the  $\text{Nd}_2\text{Fe}_{14}\text{B}$  grains could be further improved by promptly removing the  $\text{Nd}_2\text{Fe}_{14}\text{B}$  grains from the magnet anode to avoid their dissolution *via* electrochemical direct oxidation. Additionally, a novel recycling route based on electrochemical etching was proposed, which is anticipated to be more economically feasible in the long term and offers significantly greater flexibility compared to direct reuse methods.

Compared to organic electrolytes, aqueous electrolytes offer several advantages, including high solubility for metal salts, low volatility and low cost. Moreover, RE metals in the NdFeB

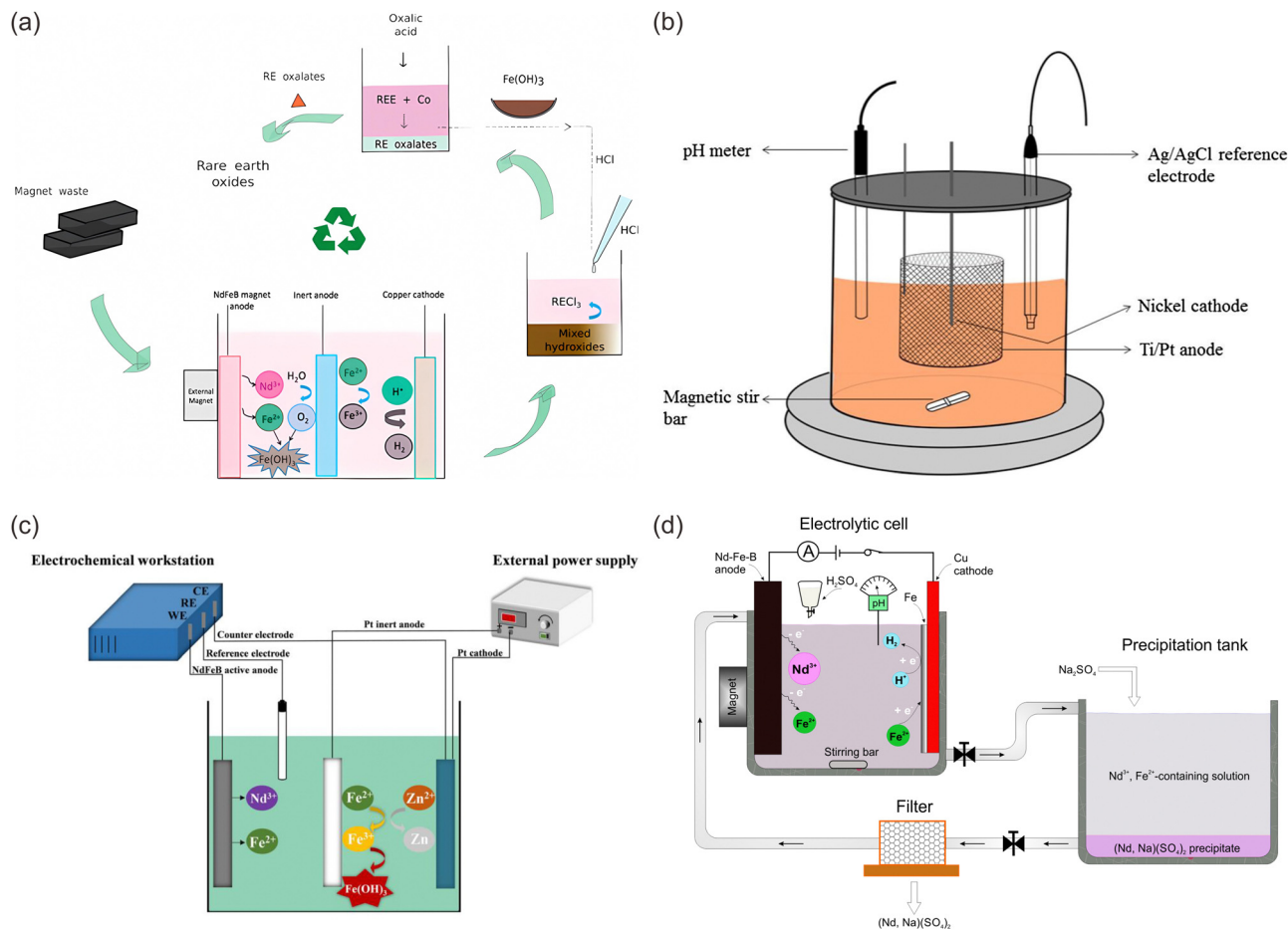


Fig. 9 Schematic representation of (a) recovering RE oxides from NdFeB magnet waste using a dual anode electrolysis reactor, (b) the electrolysis cell for *in situ* electrochemical oxidation of Fe<sup>2+</sup>, (c) a dual anode electrolysis device for recovering REEs from NdFeB magnets (CE, counter electrode; RE, reference electrode; and WE, working electrode) and (d) the closed-loop recycling route for recovering REEs from the NdFeB magnet waste. Reproduced with permission from ref. 51–54.

magnets could react spontaneously with water.<sup>50</sup> Therefore, aqueous electrolytes are suitable for recovering REEs from waste NdFeB magnets. Venkatesan *et al.*<sup>51</sup> employed a dual anode system to leach NdFeB magnets *via* electrochemical direct oxidation in a NH<sub>4</sub>Cl solution. One anode, a bulky NdFeB magnet scrap, was directly dissolved in the electrolyte by passing an electric current, while the other, a Ti/Pt inert anode, converted Fe<sup>2+</sup> dissolved from the waste magnet to Fe<sup>3+</sup> (eqn (15)) *in situ* by electrochemical oxidation (Fig. 9(a)). The electrolysis process was carried out at room temperature for 8 h (anodic dissolution current of 0.5 A, 3.0 mol L<sup>-1</sup> of NH<sub>4</sub>Cl), resulting in the dissolution of more than 97% of the REEs from the magnet. Subsequently, the REEs and Co were selectively recovered from the leach solution with 0.14 mol L<sup>-1</sup> HCl over 3 h, leaving Fe(OH)<sub>3</sub> as a residue. The REEs were then recovered by oxalic acid precipitation, followed by calcination to produce high-purity REE oxides (99%).



It is important to note that *in situ* electrochemical oxidation of Fe<sup>2+</sup> to Fe<sup>3+</sup> is an effective method that facilitates the removal of Fe in the leachate in the form of Fe(OH)<sub>3</sub>. Venkatesan *et al.*<sup>52</sup> reported that approximately 99% of Fe<sup>2+</sup> in the leach solution, obtained by completely dissolving waste NdFeB magnets, was electrochemically oxidized by applying a current of 1.2 A for 4 h in a single-chamber cell (Fig. 9(b)). In comparison, only 2% of FeCl<sub>2</sub> was oxidized to FeCl<sub>3</sub> through air bubbling over a period of 64 h. Since the anode and cathode were placed in a single chamber, the back reduction of Fe<sup>3+</sup> to Fe<sup>2+</sup> on the cathode (eqn (16)) was thermodynamically favourable. Therefore, an anode with a substantially larger surface area than the cathode was employed to promote the hydrogen evolution reaction (eqn (17)) as the primary cathodic reaction, minimizing the back-reduction of Fe<sup>3+</sup> to Fe<sup>2+</sup> on the cathode.

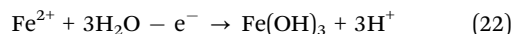
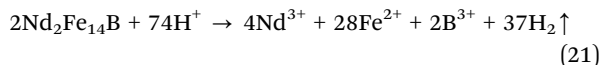
An alternative strategy to prevent the back-reduction of Fe<sup>3+</sup> to Fe<sup>2+</sup> on the cathode is to introduce a competing cathodic reaction that occurs before the reduction of Fe<sup>3+</sup> in a single-chamber cell. Zhang *et al.*<sup>53</sup> introduced a ZnCl<sub>2</sub> solution as the



Table 1 Recycling processes studied for the treatment of waste NdFeB magnets

Type of waste	Process step	Electrolyte/leaching solution	Final products	Efficiency	Purity	Energy and chemical consumption	Ref.
NdFeB scrap	Molten salt electrolysis → Water rinsing	LiF + CaF <sub>2</sub> (80 : 20 mol%, 1123 K, 0.288 A)	RE metal, FeB	90%	> 99%	—	34
NdFeB scrap	Molten salt electrolysis → Water rinsing	LiCl + KCl (58.5 : 41.5 mol%, 723 K, 0.67 V, 24 h)	RE alloy	—	—	—	35
NdFeB scrap	Room-temperature electrolysis → Magnetic separation	DMF + 0.3 mol L <sup>-1</sup> FeCl <sub>2</sub> (25 °C, 2 mA cm <sup>-2</sup> , 6 h)	Nd <sub>2</sub> Fe <sub>14</sub> B grains, Fe metal	67.2%	—	0.58 kWh kg <sup>-1</sup> , 1.52 kg FeCl <sub>2</sub> per kg	11
NdFeB scrap	Room-temperature electrolysis → Selective leaching in HCl	3 mol L <sup>-1</sup> NH <sub>4</sub> Cl (25 °C, 0.5 A, 8 h)	RE oxides, Fe(OH) <sub>3</sub>	> 97%	99.2%	2.9–3.6 kWh kg <sup>-1</sup> , 0.37 kg oxalic acid per kg	51
NdFeB scrap	→ Oxalic acid precipitation → Calcination	0.5 mol L <sup>-1</sup> citric acid (25 °C, 20 mA cm <sup>-2</sup> , 5 h)	RE oxides, Fe <sub>2</sub> O <sub>3</sub>	~ 100%	99.9%	4.6 kWh kg <sup>-1</sup> , 1.05 kg oxalic acid per kg	56
NdFeB scrap	Room-temperature electrolysis → Selective precipitation	0.4 mol L <sup>-1</sup> FeSO <sub>4</sub> + (NH <sub>4</sub> ) <sub>2</sub> SO <sub>4</sub> + 0.175 mol L <sup>-1</sup> Na <sub>3</sub> Cit + 0.4 mol L <sup>-1</sup> H <sub>3</sub> BO <sub>3</sub> (25 °C, 25 mA cm <sup>-2</sup> , 8 h)	RE double salts, Fe metal	99.9%	99.4%	1.36 kWh kg <sup>-1</sup> , 0.32 kg Na <sub>2</sub> SO <sub>4</sub> per kg	54
NdFeB scrap	Partial HCl leaching → Room-temperature electrolysis → Filtration	HCl (nHCl/nREE = 3.5) + 3.5 mol L <sup>-1</sup> NaCl (25 ± 2 °C, 125 mA cm <sup>-2</sup> , 2.5 h)	RE oxides, Fe(OH) <sub>3</sub>	> 95%	99.5%	0.34 kg H <sub>2</sub> SO <sub>4</sub> per kg, > 0.95 kWh kg <sup>-1</sup>	60
NdFeB swarf	Room-temperature electrolysis → Selective precipitation	0.6 mol L <sup>-1</sup> Fe(NH <sub>4</sub> ) <sub>2</sub> (SO <sub>4</sub> ) <sub>2</sub> + 0.175 mol L <sup>-1</sup> Na <sub>3</sub> Cit + 0.4 mol L <sup>-1</sup> H <sub>3</sub> BO <sub>3</sub> (25 °C, 20 mA cm <sup>-2</sup> , 10 h)	RE double salts, Fe metal	92.2%	98.4%	19.5 kg NaCl per kg, 0.37 kg oxalic acid per kg	12
NdFeB scrap	Oxidative roasting (950 °C, 15 h) → Acid leaching → Solvent extraction	5 mol L <sup>-1</sup> HNO <sub>3</sub> (80 °C, 72 h)	RE oxides, Fe <sub>2</sub> O <sub>3</sub> , CoO	> 99%	> 99.5%	0.33 kg Na <sub>2</sub> SO <sub>4</sub> per kg, 0.33 kg H <sub>2</sub> SO <sub>4</sub> per kg	62
NdFeB swarf	Oxidative roasting (400 °C, 2 h) → Acid leaching → Solvent extraction	6 mol L <sup>-1</sup> HCl (90 °C, 2 h)	RE oxalate, Fe oxalate	98.28%	98.39%	0.47 kg HNO <sub>3</sub> per kg, 1.6 kg NH <sub>4</sub> NO <sub>3</sub> per kg	63
NdFeB scrap	Oxidative roasting (800 °C, 2 h) → Acid leaching → Precipitation	0.6 mol L <sup>-1</sup> HCl (180 °C, 2 h)	RE oxalate, Fe <sub>2</sub> O <sub>3</sub>	99%	99.95%	3.74 kg HCl per kg, 1.04 kg oxalic acid per kg	64
NdFeB scrap	Sulfation roasting (14.5 mol L <sup>-1</sup> H <sub>2</sub> SO <sub>4</sub> , 750 °C, 1 h) → Water leaching	Water (25 °C, 1 h)	RE sulfate solution, Fe <sub>2</sub> O <sub>3</sub>	98%	99.98%	0.63 kg HCl per kg, 0.02 kg NaNO <sub>3</sub> per kg	65
NdFeB scrap	Alkali baking (10 mol L <sup>-1</sup> NaOH, 200 °C, 1.5 h) → Acid leaching → Solvent extraction → Precipitation → Calcination	20 vol% versatic acid (60 °C, 1 h)	RE oxides, Fe <sub>2</sub> O <sub>3</sub>	> 95%	98%	0.27 kg oxalic acid per kg, 4.3 kg H <sub>2</sub> SO <sub>4</sub> per kg	66

Note: "Energy and chemical consumption" was calculated based on the consumed electricity (kWh) and chemicals (kg) per kilogram of waste NdFeB magnets.



Venkatesan *et al.*<sup>60</sup> successfully recovered REEs from crushed NdFeB magnets through a two-step process involving partial leaching in HCl solution followed by electrolysis. To completely prevent the migration of  $\text{Fe}^{3+}$  to the cathode, an anion exchange membrane (AEM) was used as an effective physical barrier to divide the electrolytic reactor into a two-chamber cell (Fig. 11). Consequently,  $\text{Fe}^{2+}$  was effectively oxidized in the anodic chamber during the electrolysis process and hydrolysed as  $\text{Fe}(\text{OH})_3$  with the release of  $\text{H}^+$  (eqn (22)). The liberated  $\text{H}^+$  from the oxidation process was utilized for leaching the undissolved magnet. Therefore, the anodic redox mediator,  $\text{Fe}^{2+}/\text{Fe}^{3+}$ , could be regarded as the effective leaching agent for NdFeB swarf dissolution. Nevertheless, higher than 95% of the REEs were leached into the solution under the optimal condition (current density of  $125 \text{ mA cm}^{-2}$ ,  $3.5 \text{ mol L}^{-1}$  of anolyte NaCl and  $0.05 \text{ mol L}^{-1}$  of catholyte NaCl) and all the Fe was removed as  $\text{Fe}(\text{OH})_3$  precipitate.

The REEs present in the leaching solution were then separated by oxalic acid precipitation. The whole process consumed only NaCl, oxalic acid and electric current and produced RE oxides with a purity of  $\geq 99\%$ . Additionally, other electrochemically generated oxidants, such as hydroxyl radicals ( $\bullet\text{OH}$ ) and chlorine ( $\text{Cl}_2$ ), *etc.*, which have been applied in the dissolution of valuable metals in vanadium- and chromium-containing slag and waste printed circuit boards,<sup>61</sup> also hold potential for dissolving NdFeB swarf.

The recycling of waste NdFeB magnets through room-temperature electrolysis significantly diminishes the use of strong acids and alkalis. Nevertheless, challenges related to slow reaction rates during the dissolution of waste NdFeB magnets, precise control of both anodic and cathodic reactions, and scaling up the process remain unresolved and require further investigation. Table 1 summarizes the different electrochemical processes used for the recycling of waste NdFeB magnets.

## Conclusions and perspectives

The demand for NdFeB permanent magnets has been steadily increasing and is expected to continue to rise, primarily driven by the rapid development of wind power and electric vehicles amid the global green and low-carbon transition. The growing demand for NdFeB magnets, coupled with the limited supply of RE resources, will likely lead to a supply gap for Nd and Pr, which are key REEs for producing NdFeB magnets. Recycling waste NdFeB magnets presents a promising strategy to mitigate this supply gap and support sustainable economic growth.

Current recycling methods largely rely on metallurgical processes that involve extreme reaction conditions and significant chemical consumption, leading to considerable solid and liquid waste generation. Electrochemical recovery offers a more

environmentally friendly alternative. Electrochemical recycling of waste NdFeB magnets provides a novel pathway to improve recycling outcomes by eliminating waste generation, fostering technological innovations, and achieving high recovery efficiency. Molten salt electrolysis can selectively dissolve REEs from both NdFeB magnet scraps and swarf through direct anodization and flux extraction process, respectively and ends up with the products of RE metals and FeB alloys. These products could be directly used in new magnet manufacturing. Room-temperature electrolysis can be applicable to both NdFeB magnet scraps and swarf, using organic electrolytes and aqueous electrolytes to recover  $\text{Nd}_2\text{Fe}_{14}\text{B}$  grains and REEs, respectively. The recovered  $\text{Nd}_2\text{Fe}_{14}\text{B}$  grains hold potential for high-performance magnet production, while the recovered REEs could be used in other high-tech applications beyond permanent magnets.

However, the electrochemical processes for recycling waste NdFeB magnets are still in their early stages. Challenges such as suboptimal current efficiency and electrode stability require further research to develop more practical and efficient electrochemical strategies. This paper provides the following opportunities to advance the electrochemical recycling of waste NdFeB magnets:

(1) Environmental and economic evaluation of entire recycling processes: despite the relative simplicity of electrochemical recycling routes, the final products are typically RE alloys or compounds. A systematic assessment of the potential environmental impacts of the entire process is necessary, accounting for emissions and energy consumption.

(2) High-efficiency electrochemical leaching: aqueous electrolyte-based REE recovery is often limited by mass transport. Electrochemically generated oxidants, such as hydroxyl radicals ( $\bullet\text{OH}$ ) and chlorine ( $\text{Cl}_2$ ), with strong oxidizing capacities, could potentially enhance leaching kinetics.

(3) Rational design of novel recycling route with reduced reagent consumption: current electrochemical recycling methods mainly target NdFeB scraps, with insufficient attention given to heavily contaminated NdFeB swarf. Furthermore, substantial amounts of strong acids and alkalis are still required to deeply separate REEs from Fe. Proper utilization of the *in situ* anode-generated  $\text{H}^+$  and cathode-generated  $\text{OH}^-$  may offer a viable alternative to reduce the chemical consumption.

## Author contributions

X. Xu wrote the original draft, X. Jia, K. Zhao, P. Xu and B. Liu collected textual and diagram information, P. Jing and J. Zhang reviewed and edited the manuscript.

## Data availability

No primary research results, software or code have been included and no new data were generated or analysed as part of this review.

## Conflicts of interest

There are no conflicts to declare.

## Acknowledgements

This work was supported by the National Natural Science Foundation of China (52304425 and 22361033), the “Inner Mongolia Autonomous Region 2022 Leading Talent Team of Science and Technology” Program (2022LJRC0008), the Program for Innovative Research Team in Universities of Inner Mongolia Autonomous Region (NJYT23031), the “Grassland Leading Talent” Program of Inner Mongolia, the “Grassland Talent” Innovation Team of Inner Mongolia, the 111 Project (D20033) and the Program of Higher-level Talents of IMU (10000-21311201/052).

## References

- European Commission, Critical raw materials for strategic technologies and sectors in the EU – A foresight study, <https://ec.europa.eu/docsroom/documents/42881>, (accessed June 20, 2024).
- International Energy Agency, Net zero by 2050: A roadmap for the global energy sector, <https://www.iea.org/reports/net-zero-by-2050>, (accessed June 20, 2024).
- International Energy Agency, The role of critical minerals in clean energy transitions, <https://www.iea.org/reports/the-role-of-critical-minerals-in-clean-energy-transitions>, (accessed June 20, 2024).
- Arafura Rare Earths Limited, Supply and demand, <https://www.arultd.com/products/supply-and-demand/>, (accessed June 20, 2024).
- U.S. Geological Survey, Rare earth, 2024, <https://pubs.usgs.gov/periodicals/mcs2024/mcs2024-rare-earth.pdf> (accessed December 4, 2024).
- T. Xu, X. Zheng, B. Ji, Z. Xu, S. Bao, X. Zhang, G. Li, J. Mei and Z. Li, *Sep. Purif. Technol.*, 2024, **330**, 125501.
- X. Yin, L. P. Ang and Z. Y. Chang, *Science*, 2024, **384**, 1182.
- M. Reimer, H. Schenk-Mathes, M. Hoffmann and T. Elwert, *Metals*, 2018, **8**, 867.
- Z. Zhihan, W. Zhi, W. Dong, L. Yong, X. Wanhai, L. Chenghao, L. Yang, W. Jian and L. Guobiao, *Sep. Purif. Technol.*, 2023, **315**, 123654.
- G. Yu, S. Ni, Y. Gao, D. Mo, Z. Zeng and X. Sun, *Hydrometallurgy*, 2024, **223**, 106209.
- X. Xu, S. Sturm, Z. Samardzija, J. Vidmar, J. Scancar and K. Zuzek Rozman, *ChemSusChem*, 2019, **12**, 4754–4758.
- X. Xu, X. Jia, P. Jing, Y. Zhang, J. Cui, K. Zuzek, S. Saso, B. Liu and J. Zhang, *J. Rare Earths*, 2024, DOI: **10.1016/j.jre.2024.02.001**.
- E. H. Lalana, M. J. Degri, A. Bradshaw and A. Walton, *The European Powder Metallurgy Association*, 2016, pp. 1–6.
- C. Jonsson, M. Awais, L. Pickering, M. Degri, W. Zhou, A. Bradshaw, R. Sheridan, V. Mann and A. Walton, *J. Cleaner Prod.*, 2020, **277**, 124058.
- S. Shirayama and T. H. Okabe, *Metall. Mater. Trans. B*, 2018, **49**, 1067–1077.
- T. Lorenz and M. Bertau, *J. Cleaner Prod.*, 2019, **215**, 131–143.
- M. Moore, A. Gebert, M. Stoica, M. Uhlemann and W. Löser, *J. Alloys Compd.*, 2015, **647**, 997–1006.
- M. Sun, X. Hu, L. Peng, P. Fu, W. Ding and Y. Peng, *J. Mater. Process. Technol.*, 2015, **218**, 57–61.
- O. Takeda, K. Nakano and Y. Sato, *Mater. Trans.*, 2014, **55**, 334–341.
- Y. Bian, S. Guo, L. Jiang, K. Tang and W. Ding, *J. Sustain. Metall.*, 2015, **1**, 151–160.
- S. T. Abrahimi, Y. Xiao and Y. Yang, *Miner. Process. Extr. Metall.*, 2015, **124**, 106–115.
- Z. Zhihan, W. Dong, L. Chenghao, Z. Wang, X. Wanhai, Q. Guoyu and L. Guobiao, *J. Environ. Chem. Eng.*, 2022, **10**, 108946.
- Y. Jiang, Y. Deng, W. Xin and C. Guo, *Trans. Indian Inst. Met.*, 2020, **73**, 703–711.
- K. Binnemans, P. T. Jones, B. Blanpain, T. Van Gerven, Y. Yang, A. Walton and M. Buchert, *J. Cleaner Prod.*, 2013, **51**, 1–22.
- G. S. Frankel, *J. Electrochem. Soc.*, 1998, **145**, 2186.
- M. Stefanoni, U. M. Angst and B. Elsener, *Nat. Mater.*, 2019, **18**, 942–947.
- A. D. Bas, E. Ghali and Y. Choi, *Hydrometallurgy*, 2017, **172**, 30–44.
- P. K. Katiyar and N. S. Randhawa, *Int. J. Refract. Met. Hard Mater.*, 2020, **90**, 105251.
- A. Schreiber, J. Marx, P. Zapp and W. Kuckshinrichs, *Adv. Eng. Mater.*, 2020, **22**, 1901206.
- D. C. Harris, in *Quantitative chemical analysis*, W. H. Freeman, 8th edn, 2010.
- Y. Kamimoto, T. Itoh, K. Kuroda and R. Ichino, *J. Mater. Cycles Waste Manage.*, 2017, **19**, 1017–1021.
- A. M. Martinez, O. Kjos, E. Skybakmoen, A. Solheim and G. M. Haarberg, *ECS Trans.*, 2013, **50**, 453–461.
- Y. Kamimoto, T. Itoh, G. Yoshimura, K. Kuroda, T. Hagio and R. Ichino, *J. Mater. Cycles Waste Manage.*, 2018, **20**, 1918–1922.
- Y. Yang, C. Lan, L. Guo, Z. An, Z. Zhao and B. Li, *Sep. Purif. Technol.*, 2020, **233**, 116030.
- H. Konishi, H. Ono, E. Takeuchi, T. Nohira and T. Oishi, *ECS Trans.*, 2014, **64**, 593–600.
- A. Abbasalizadeh, L. Teng, S. Sridhar and S. Seetharaman, *Miner. Process. Extr. Metall.*, 2015, **124**, 191–198.
- S. G. Heo, J. Y. Yang, S. J. Oh, S. J. Seo, M. H. Lee and K. T. Park, *J. Rare Earths*, 2024, DOI: **10.1016/j.jre.2024.01.012**.
- A. Abbasalizadeh, A. Malfliet, S. Seetharaman, J. Sietsma and Y. X. Yang, *Mater. Trans.*, 2017, **58**, 400–405.
- D. Shen and R. Akolkar, *J. Electrochem. Soc.*, 2017, **164**, H5292.
- S. Park, D. K. Kim, J. Jeong, J. H. Shin, Y. Kang, R. Liu, T. S. Kim and M. Song, *J. Alloys Compd.*, 2023, **967**, 171775.
- Z. Xu, L. Jia, Z. He, X. Guo and Q. Tian, *Trans. Nonferrous Met. Soc. China*, 2024, **34**, 1634–1654.
- O. Takeda, T. Uda and T. H. Okabe, in *Treatise on Process Metallurgy*, Elsevier, 2nd edn, 2014, pp. 995–1044.
- Z. Hua, J. Wang, L. Wang, Z. Zhao, X. Li, Y. Xiao and Y. Yang, *ACS Sustainable Chem. Eng.*, 2014, **2**, 2536–2543.
- Y. Jeon, J. Hur, G. Y. Jeong, S. Sohn and J. Park, *J. Alloys Compd.*, 2021, **860**, 158424.
- A. Abbasalizadeh, A. Malfliet, S. Seetharaman, J. Sietsma and Y. Yang, *J. Sustain. Metall.*, 2017, **3**, 627–637.
- J. Holc, S. Beseničar and D. Kolar, *J. Mater. Sci.*, 1990, **25**, 215–219.
- S. Mao, H. Yang, Z. Song, J. Li, H. Ying and K. Sun, *Corros. Sci.*, 2011, **53**, 1887–1894.
- S. Mao, H. Yang, J. Li, F. Huang and Z. Song, *Appl. Surf. Sci.*, 2011, **257**, 5581–5585.
- A. A. El-Moneim, A. Gebert, F. Schneider, O. Gutfleisch and L. Schultz, *Corros. Sci.*, 2002, **44**, 1097–1112.
- G. Yan, P. J. McGuinness, J. P. G. Farr and I. R. Harris, *J. Alloys Compd.*, 2009, **478**, 188–192.
- P. Venkatesan, T. Vander Hoogerstraete, K. Binnemans, Z. Sun, J. Sietsma and Y. Yang, *ACS Sustainable Chem. Eng.*, 2018, **6**, 9375–9382.
- P. Venkatesan, Z. H. I. Sun, J. Sietsma and Y. X. Yang, *Sep. Purif. Technol.*, 2018, **191**, 384–391.
- Z. Zhang, Z. Wang, D. Wang, R. Min, W. Xiao, Y. Lin and G. Li, *Green Chem.*, 2023, **25**, 10653–10663.
- X. Xu, S. Sturm, Z. Samardzija, J. Scancar, K. Markovic and K. Zuzek Rozman, *Green Chem.*, 2020, **22**, 1105–1112.
- I. Makarova, J. Ryl, Z. Sun, I. Kurilo, K. Gornicka, M. Laatikainen and E. Repo, *Sep. Purif. Technol.*, 2020, **251**, 117362.
- A. Kumari, Dipali, N. S. Randhawa and S. K. Sahu, *J. Cleaner Prod.*, 2021, **309**, 127393.
- M. Yue, X. Yin, X. Li, M. Li, X. Li, W. Liu, Y. Wu, D. Zhang, J. Chen and X. Yi, *ACS Sustainable Chem. Eng.*, 2018, **6**, 6547–6553.

- 58 E. Padhan, A. K. Nayak and K. Sarangi, *Hydrometallurgy*, 2017, **174**, 210–215.
- 59 X. Xu, J. Gao, K. Zhao, H. Sun, P. Jing, B. Liu and J. Zhang, *Green Chem.*, 2024, **26**, 2552–2559.
- 60 P. Venkatesan, T. Vander Hoogerstraete, T. Hennebel, K. Binnemans, J. Sietsma and Y. X. Yang, *Green Chem.*, 2018, **20**, 1065–1073.
- 61 Y. Xue and Y. Wang, *Green Chem.*, 2020, **22**, 6288–6309.
- 62 S. Riaño and K. Binnemans, *Green Chem.*, 2015, **17**, 2931–2942.
- 63 Z. Liu, H. Zhou, W. Li, X. Luo, J. Wang and F. Liu, *Sep. Purif. Technol.*, 2022, **282**, 119795.
- 64 F. Liu, A. Porvali, J. Wang, H. Wang, C. Peng, B. P. Wilson and M. Lundström, *Miner. Eng.*, 2020, **145**, 106097.
- 65 M. A. R. Önal, C. R. Borra, M. Guo, B. Blanpain and T. Van Gerven, *J. Sustain. Metall.*, 2015, **1**, 199–215.
- 66 M. A. R. Önal, S. Riaño and K. Binnemans, *Hydrometallurgy*, 2020, **191**, 105213.